

# Computational Modeling and Analysis of the Effects of Retinal Injury on the Formation of Response Feature Maps in the Primary Visual Cortex

Robert Chen

## Abstract

Retinal diseases impair vision, making the visual field appear blurry. As a result, properties of visual stimuli are manipulated. The representation of response features of neurons in the primary visual cortex (V1) changes as well. In this investigation, the Kohonen self-organizing map algorithm was used to model the formation of response feature maps under normal conditions as well as under diseased conditions. The following response features were included in the computational models: retinotopy, orientation preference, orientation selectivity, spatial frequency, and ocular dominance. In injured maps formed with disease of radius 2.5 retinotopic units (2.5 pixels, same length as the retinotopy tuning width), gradient magnitude comparison showed no significant difference in the feature maps of normal and injured conditions for maps of orientation selectivity, orientation preference, and ocular dominance. Furthermore, continuity was retained in all maps formed under disease of radii 5 units and 2.5 units. These observations suggest that retinal diseases with radii close in length to the retinotopy tuning width may not create a significant impact on response feature map formation. Also, it was demonstrated that in cases of retinal injury, the visual cortex is able to reorganize itself in areas of the visual cortex analogous to injured areas of the retina. In addition, response feature map formation was modeled for a condition in which stimuli values for orientation selectivity and spatial frequency were chosen from a weighted probability distribution using a Monte Carlo sampling method.

## 1 Introduction

Computational models can be used to simulate the interactions between neurons in specific parts of the brain; these computational models help us gain insight on the ways in which the brain operates. Many computational models analyze the neocortex, the area of the brain involved in high-level functions such as sensory perception, spatial reasoning, and conscious thought [8]. The primary visual cortex, the area of the neocortex which receives visual input from the retina, is of particular interest.

The primary visual cortex (V1) is one of five main areas of the visual cortex. After V1 receives visual input from the retina, it transmits the information primarily to two pathways: the ventral stream, which is associated with form recognition and object representation (i.e. form vision) and the dorsal stream, which is associated with motion and representation of object locations (i.e. spatial vision) [13]. The neurons in the V1 region act as receptive fields for visual stimuli which are transduced by the retina and relayed to the primary visual cortex. In the brain, the V1 region exists as an intricately folded sheet of interconnected neurons. However, for the purposes of computational modeling, the region is represented by an “unfolded” two-dimensional sheet of neurons.

Neurons in V1 fire after receiving visual input from the retina; each neuron fires at a different intensity in response to a specific stimulus. Cortical maps of neuron firing intensities can be formed. A dimension-reduction model helps explain the organization of neurons according to their response properties. Dimension-reduction models seek to map multi-dimensional cortical response features (e.g. response features to visual stimuli) to a simpler, two-dimensional area. One significant goal of many dimension-reduction models is to bring closer the neighboring neurons which share similar properties [3, 6]. This is achieved by reducing the connection length between neurons. Cortical feature maps are formed based on the intensity of responses to visual input from the retina. Response features which are coded in V1 include: azimuth retinotopic position, elevation retinotopic position, orientation selectivity, orientation preference, ocular dominance, and spatial frequency preference<sup>1</sup>.

The mapping of response features on the neocortex is simulated by a self-organizing map.

This is a neural network which provides a visual representation in low dimensions (usually 2 or 3 dimensions) for topological properties which may involve several dimensions [4]. Self-organizing maps are commonly used for modeling of the visual cortex because they selectively update the neurons in the neighborhood region of a given neuron, thus working under the dimension-reduction model. A self-organizing map of V1 gives a representation of the visual field as seen through the eyes.

The stimuli and response features represented in the self-organizing map work to model data from real-life electrophysiological experiments, primarily involving ferret and cat V1 regions. Response feature maps are created via optical imaging of intrinsic signals [5].

Although computational models have been developed for a variety of situations involving cat and ferret V1 regions [3, 6, 7, 10–12], they do not take into account possible situations involving retinal pathology. Retinal diseases involve blurring of vision in certain areas of the visual field. Retinal diseases directly impact the spatial frequency and orientation selectivity response features, as these features are involved in changing the clarity of vision perceived through the retina. Examples of retinal diseases include glaucoma and macular degeneration. Glaucoma involves blurriness in peripheral vision while macular degeneration involves blurriness in certain spots across the visual field.

In this study, computational models for retinal injury were developed and implemented with the computational model of the cortical response feature maps. Several cases involving the retinal injury model were implemented with the self-organizing map algorithm, and it was found that cortical maps can “repair”<sup>2</sup> themselves only if small areas of the retina were affected by the disease (mapping is changed for areas of the visual cortex analogous to the injured region of the retina). In these disease cases, the cortex does not receive visual input from certain areas of the visual field.

Furthermore, it was hypothesized that representation of orientation selectivity and spatial frequency would be different between normal and injured maps (due to blurriness of vision in retinal disease, which implies a reduced ability to discern objects of high orientation selectivity and spatial frequency). This condition was modeled with a Monte Carlo (MC) distribution of stimulus values for the features of orientation selectivity and spatial frequency. In the MC disease case, the cortex receives visual input from the entire visual field; however, there was not a uniform distribution of stimulus values for the aforementioned features (relatively low stimulus values for orientation selectivity and spatial frequency are presented more than are higher values).

## 2 Methods

### 2.1 Computational Model - Formation of Cortical Maps

For this investigation, a modified version of the Kohonen self-organizing map algorithm was used [3]. Each stimulus and each receptive field are represented as multicomponent vectors. It is assumed that the stimuli and receptive fields exist in a multi-dimensional feature space.

Let  $x$  represent the azimuth retinotopic position;  $y$ , elevation retinotopic position;  $q$ , orientation selectivity;  $\phi$ , orientation preference;  $z$ , ocular dominance; and  $f$ , spatial frequency preference.

Each stimulus is represented by the vector

$$V_S = (x_S, y_S, q_S \cos(2\Theta_S), q_S \sin(2\Theta_S), z_S, f_S).$$

The stimuli are mapped onto a cortical surface, where each neuron and its receptive field is represented by the vector

$$V_r = (x_r, y_r, q_r \cos(2\phi_r), q_r \sin(2\phi_r), z_r, f_r).$$

In these vectors, the feature  $x$  ranges from  $(0, X)$ ,  $y$  from  $(0, Y)$ ,  $q$  from  $(0, Q)$ ,  $\phi$  from  $(0, \pi)$ ,  $z$  from  $(0, Z)$ , and  $f$  from  $(0, F)$ . The stimuli are mapped onto a cortical surface with dimensions  $N \times N$ . Each cortical point was identified as  $r = (i, j)$ . At the beginning of the simulation, the following parameters were set:  $x_r = i$ ,  $y_r = j$ ,  $q_r = Q/2$ ,  $\phi_r = \pi/2$ ,  $z_r = Z/2$ , and  $f_r = F/2$ .

To form the maps, iterations of three steps each are performed. (1) A stimulus is chosen at random from the feature space. (2) The cortical point whose features are most similar to those of the stimulus is identified as the “winner neuron”. The winner neuron is determined by finding the neuron which is closest to the stimulus in terms of Euclidean distance. Euclidean distance was determined by the expression  $|V_S - W_r|^2$ . (3) The winner neuron and the neurons around it are updated by the equation

$$\Delta W_r = \alpha h(r)(V_S - W_r),$$

where  $\alpha$  is the learning rate,  $r$  is the cortical distance between the winner neuron and any given cortical point  $(i, j)$ , and  $h(r)$  is the neighborhood function. The neighborhood function modifies all neurons on the cortical map. The neurons closest (in terms of cortical distance) to the winner neuron are

updated the most, while neurons farther away from the winner are updated less. The neighborhood function is

$$h(r) = e^{-r^2/\sigma^2}$$

which restricts modifications in receptive fields to cortical points nearby the winner. Usually, the neighborhood function modifies only the area within a radius of  $\sigma$  (in terms of cortical distance) from the winner neuron.  $\sigma$  is referred to as the retinotopy tuning width.

The following parameters were used for the simulation:  $N=65$ ,  $\sigma = 2.5$ ,  $\alpha = 0.02$ ,  $X = N$ ,  $Y = N$ ,  $Q = 10$ ,  $Z = 15$ ,  $F = 15$ . 100,000 iterations of the algorithm were completed. Periodic boundary conditions were implemented for all cortical maps. Each pixel was analogous to one cortical neuron and each pixel represented one retinotopic unit. The resulting map represented a 65 x 65 sheet of neurons.

## 2.2 Computational Model - Retinal Injury

Two different disease cases were implemented in this study. Both disease cases model the reorganization of the cortical maps after injury in areas of the retina. For all disease simulations, the same parameters as those used in creating the normal maps were used. All disease simulations were run for 100,000 iterations. In generating the response feature maps, results were averaged over 10 simulations, using a different random number seed for each simulation. For disease cases 1 and 2, a uniform probability distribution of stimulus values for all response features is assumed.

### 2.2.1 Disease Case 1: Center

Case 1 simulates damage to the center of the retina. A circular area in the center of the visual field does not receive input (the circular area about the cortical point  $r(33,33)$ ). Case 1 uses the same method of map formation as that of the formation of the original cortical maps (see section 2.1). Case 1 was run using the following possible radii: 2.5, 5, 10, 15, 20 units.

### 2.2.2 Disease Case 2: Scattered

Case 2 simulates damage to several areas of the retina. Circular areas on the retina do not receive visual input. Areas affected are the circular areas within a given radius from cortical points  $r(16, 16)$ ,  $r(16, 49)$ ,  $r(49, 16)$ ,  $r(49, 49)$ , and  $r(33, 33)$ . Otherwise, the Case 2 simulation was run under the same conditions as was the normal simulation. Case 2 was run using the following possible radii: 2.5, 5, 15, and 20 units.

### 2.2.3 Disease with Monte Carlo (MC) Stimulus Sampling

It was predicted that during advanced forms of retinal disease, the eye is unable to discern stimuli with high orientation selectivity and spatial frequency (properties which contribute to the clarity of visual stimuli). The MC disease case models a highly advanced form of retinal disease (as in macular degeneration), in which all associated V1 neurons are affected.

To account for the inability of the visual cortex to register stimuli with high values for these features, a Gaussian normal distribution was used to select stimulus values. The stimulus probability distribution was given by

$$p(v) = \left| \frac{e^{-x^2/2\sigma^2}}{\sigma\sqrt{2\pi}} \right|$$

where  $p(v)$  represents the probability of choosing a stimulus parameter of  $v$ . For orientation selectivity,  $\sigma = 3$ ; for spatial frequency,  $\sigma = 5$ . Uniform sampling of stimuli values was used for the following properties: retinotopy, orientation preference, and ocular dominance.

## 2.3 Analysis of Cortical Response Feature Maps

Gradient analysis was performed on the cortical maps. Gradient maps were computed for the response features of orientation preference, orientation selectivity, ocular dominance, and spatial frequency. The gradient vector magnitude for each cortical point was calculated with the expression

$$\sqrt{dx^2 + dy^2}$$

If  $A(x,y)$  represents the gradient value at the pixel  $(x,y)$ ,  $\delta x = ((A(x+1), y) - A(x, y))$  while  $\delta y = (A(x, y+1) - A(x, y))$ . To quantitatively assess the affect of the retinal disease cases on the formation of response feature maps, affected areas of the injured maps were compared against the corresponding areas of normal maps. T-tests were conducted to assess the differences between normal and injured maps for both disease cases and all disease radii. For the t-tests<sup>3</sup>, the difference in average gradient magnitude was analyzed for the affected areas of the injured map and the corresponding areas of the normal map. For example, for disease case 1, with a disease of radius of 15, the gradient magnitudes in the circular area lying in the center of the map with radius 15 pixels would be compared with the gradient magnitudes in the analogous area of the normal map.

Gradient relationships between the organizations of normal and injured maps were plotted. A significant difference between normal and injured maps is represented by a strong negative correlation between the gradient percentile of the normal map and the number of pixels of the injured map per each percentile bin. A strong negative correlation signifies that the maps of the two features being analyzed intersect at near-perpendicular angles (hence the inverse relationship). Gradient relationships between maps of different features were analyzed as well. For gradient relationships analyzed, power regression was performed to compare the strength of correlations between normal and affected maps (disease case 1 and 2) and between different feature representations during disease modeled by Monte Carlo disease stimuli sampling.

**Coverage uniformity** ( $c'$ ) was calculated for all maps.  $c'$  was defined as follows. Let  $n_{i,j} \in \{-1, 1\}$  be the ocular dominance value of cortical point  $(i, j)$ ;  $m_{i,j} \in \{-1, 1\}$  be the

<sup>3</sup> See Appendix B

spatial frequency value;  $\theta_{ij}$  the orientation preference in degrees and  $x_{ij}, y_{ij}$  the receptive field position in degrees of visual angle. Let the vector  $v = (n_s, m_s, \theta_s, x_s, y_s)$  represent a particular stimulus, and let the vector  $w_{ij} = (n_{ij}, m_{ij}, \theta_{ij}, x_{ij}, y_{ij})$  represent the center receptive field values of cortical point  $(i, j)$ . The total amount of activity,  $A$ , evoked in the cortex by a stimulus  $v$ , can be written as

$$A(v) = \sum_{i,j \in C} f(v - w_{i,j})$$

where  $f$  defines the receptive field of point  $(i,j)$  (i.e. the amount of activity evoked as a function of the difference between the stimulus value and the center receptive field values. Next, let  $n = n_s - n_{ij}$ ,  $m = m_s - m_{ij}$ ,  $\theta = \theta_s - \theta_{ij}$ ,  $x = x_s - x_{ij}$ , and  $y = y_s - y_{ij}$ . The receptive field was defined as

$$f(n, m, q, x, y) = g(n)g(m)e^{-q^2/2s_q^2}e^{-(x^2+y^2)/2s_r^2}$$

where  $g(n) = 1$  if  $n = 0$  and  $g(n) = 0$  if  $n \neq 0$ .  $\sigma_\theta$  and  $\sigma_r$  define the orientation tuning width and the retinotopy tuning width, respectively.  $A(v)$  was calculated for a representative set of stimulus values and then coverage uniformity was calculated as  $c' = \text{standard deviation}(A) / \text{mean}(A)$ .

Values of  $A$  were calculated for all combinations of  $n_s \in \{-1, 1\}$ ,  $m_s \in \{-1, 1\}$ ,  $\theta_s \in \{0, 30, 60, 90, 120, 150\}$ ,  $x_s \in \{1, 5, 9 \dots i_{\max}\}$ ,  $y_s \in \{1, 5, 9 \dots j_{\max}\}$ , where  $i_{\max}$  and  $j_{\max}$  are the size in pixels of the map (65 pixels).

Good coverage uniformity is shown by a small value for  $c'$ . A small  $c'$  value shows that the total amount of activity evoked by the visual cortex is relatively independent of the particular combination of values (i.e. all response features are mapped evenly across the cortex) [14].

### 3 Results

Quantitative analysis involving the comparison of gradient magnitudes was conducted for all response features in all disease settings. However, in the results section, only the

maps for orientation selectivity are presented for all disease situations (Figure 2). It should be noted that the maps of orientation preference, spatial frequency, and ocular dominance all exhibited similar graphical differences in response to retinal injury as did the map of orientation selectivity.

#### 3.1 Normal Conditions

Under normal conditions, the cortical maps exhibit excellent continuity (Figure 1).

#### 3.2 Disease Case 1: Center

The formation of feature maps was simulated in the presence of retinal injuries with radii of 2.5, 5, 10, and 20 units. Cortical maps that were simulated with retinal injuries of radius 10, 15, and 20 units were significantly different from cortical maps simulated in the presence retinal injuries of radius 2.5 units and injuries of radius 5 units. Orientation selectivity maps that were simulated with retinal injuries of radius 2.5 and radius 5 show properties that are similar to the maps formed under normal conditions, suggesting the ability of the visual cortex to reorganize to normal conditions. Cortical maps that were simulated with larger areas of retinal injury did not reform to their normal states. For example, (Figure 2, C) shows that a major portion of the orientation selectivity map analogous to the diseased area of the retina remained the same color as during initial conditions.

Tables 1-4<sup>4</sup> show the differences between gradient magnitudes of injured and normal maps for each disease size. Results of unpaired t-tests show that for disease radii 5 and 15, all features exhibited significantly different gradient magnitudes between the normal and injured feature maps. For disease radius 2.5, only the spatial frequency map exhibited significantly different gradient magnitudes from the normal map.

When gradient relationships between the affected areas of injured and normal maps (see Methods section), a clearly negative correlation was observed in all response features for disease radius 15. For disease radius 5 and 2.5, plots for

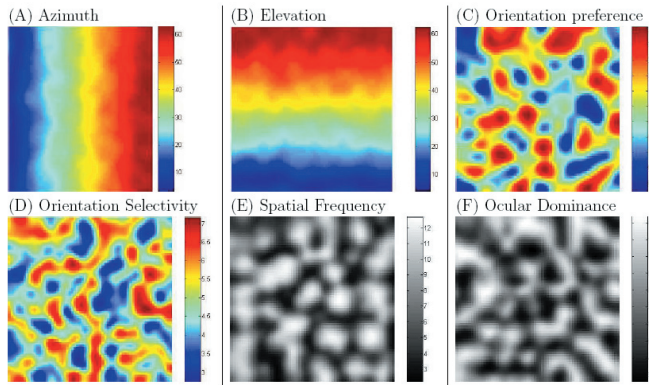


Figure 1: Response feature maps under normal conditions. (A) Azimuth position preference map. (B) Elevation position preference map. (C) Orientation preference map, which ranges from 0 radians to  $\pi$  radians. (F) Low values for ocular dominance indicate preference for contralateral eye, while high values indicate preference for ipsilateral eye.

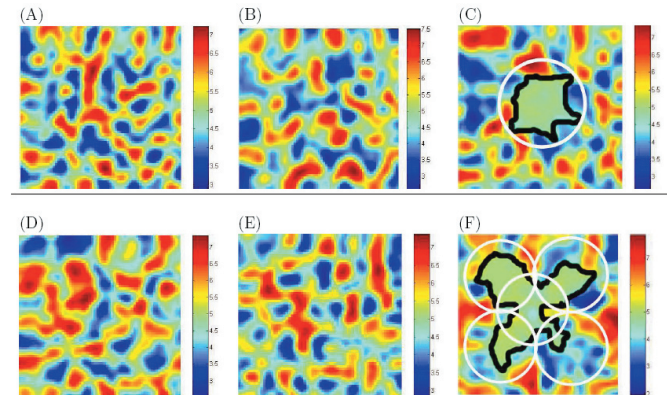


Figure 2: Maps of orientation selectivity formed in disease case 1 (A-C) and disease case 2 (D-F). Maps were formed with disease areas of radius 2.5 (A, D), 5 (B, E), 10 (C, F). Areas of the cortical maps unable to reform after retinal disease are outlined in (C, F). The areas of the maps analogous to injured areas of the retina are outlined in white (C, F).



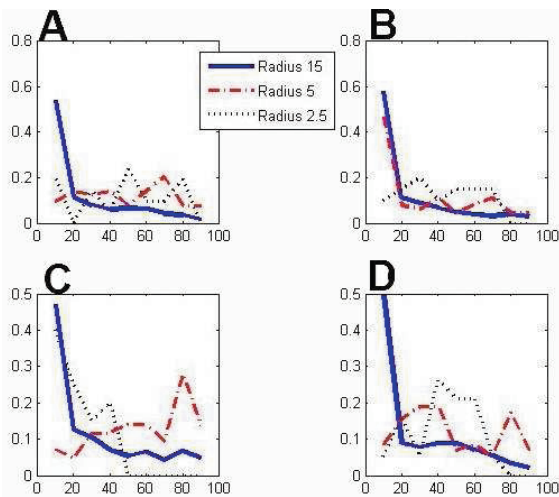


Figure 3: Disease Case 1: Pixels of normal map are grouped into ten bins according to their gradient percentile (x-axis), and the percentage of pixels of the injured map for each percentile group is indicated (y-axis, shown as a fractional value out of 1). A: Orientation selectivity; B: Orientation preference; C: Spatial frequency; D: Ocular dominance.

orientation selectivity, orientation preference, and ocular dominance did not show a clear relationship. However, a weak correlation was observed in the spatial frequency plots for disease radius 5 and 2.5, suggesting that the spatial frequency feature is strongly affected by retinal disease, even in cases of small disease size.

### 3.3 Disease Case 2: Scattered

The formation of cortical response feature maps was simulated with retinal injuries with radii of 2.5, 5, and 20 units. Cortical maps that were simulated with retinal injuries of radius 15 units were significantly different from cortical maps simulated with retinal injuries of radius 2.5 units and radius 5 units (Figure 2 D-F).

The map of orientation selectivity with retinal injury of radius 15 was able to form with a smaller affected area than the initial affected area. However, the injured area did not reform completely, as parts of the affected areas retained the same color as during initial conditions. Also, the affected area of the area of the cortical map was not uniform (Figure 2, F). The injured area around the point  $r(49, 49)$  reorganized to a greater extent than the injured areas around the other injury center points.

Tables 5-8<sup>5</sup> show the differences between gradient magnitudes of injured and normal maps for each disease case. As with disease case 1, spatial frequency did not show a significant difference between gradient magnitudes of normal and injured maps; all other features exhibited a significant difference between gradient magnitudes normal and injured maps. This observation is paralleled by the plotting of gradient relationship between normal and injured maps for spatial frequency, which shows that the gradient relationship is similar for all disease sizes. Plots for all other features show that normal and injured maps are significantly different for disease radius 15; for disease radius 2.5 and 5, no clear cor-

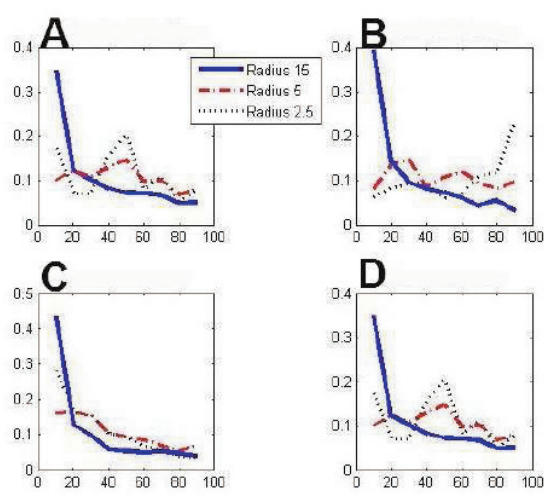


Figure 4: Disease Case 2: Pixels of normal map are grouped into ten bins according to their gradient percentile (x-axis), and the percentage of pixels of injured map for each percentile group is indicated (y-axis, shown as a fractional value out of 1). A: Orientation selectivity; B: Orientation preference; C: Spatial frequency; D: Ocular dominance.

relation suggested a significant difference between normal and injured maps (figure 4). For spatial frequency plots, maps from all disease sizes exhibited strong negative correlations between gradient percentile of normal maps and affected percent gradient values per normal percentile bin (power regression;  $r^2 > 0.900$  for all disease sizes). For the features of orientation selectivity, orientation preference, and ocular dominance, the plots implied strong differences between gradient percentile plots of normal and affected maps for disease radius 15 only ( $r^2 = 0.8038, 0.8770$ , and  $0.9552$ , respectively).

### 3.4 Gradient relationships between response features: case 2

Plotting gradient relationships between different response features, it was shown that spatial frequency and ocular dominance maps do not coincide with each other in a clear relationship. In the normal map, it is suggested that the maps of orientation selectivity and spatial frequency tend to intersect at near-perpendicular angles. The same observation is supported for the following combinations of features: orientation preference vs. orientation selectivity, orientation selectivity vs. ocular dominance (Figure 5).

The plot of orientation preference vs. orientation selectivity is similar in all situations, which suggests that the relationship between orientation preference and orientation selectivity remain unchanged after retinal injury. On the other hand, the plot of orientation selectivity vs. spatial frequency for radius 15 is significantly different from the plots for radius 2.5, radius 5, and normal map. A similar observation was found in the plot of orientation selectivity vs. ocular dominance. Therefore, it is suggested that the relationship between orientation selectivity and spatial frequency as well as the relationship between orientation selectivity and ocular dominance are changed during advanced levels of retinal injury (Figure 5).

<sup>5</sup> See Appendix B

<sup>6</sup> See Appendix C for maps of other response features

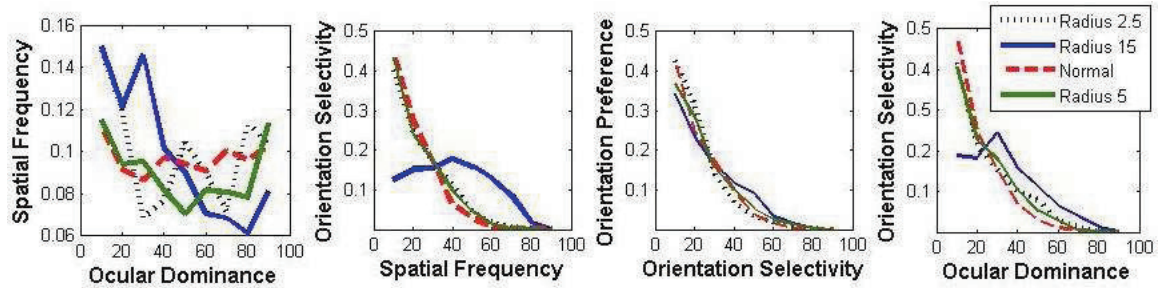


Figure 5: Disease Case 2: Pixels of one specific feature map are grouped into ten bins according to their gradient percentile (x-axis), and the percentage of pixels (of a different feature map) for each percentile group is indicated (y-axis, shown as a fractional value out of 1).

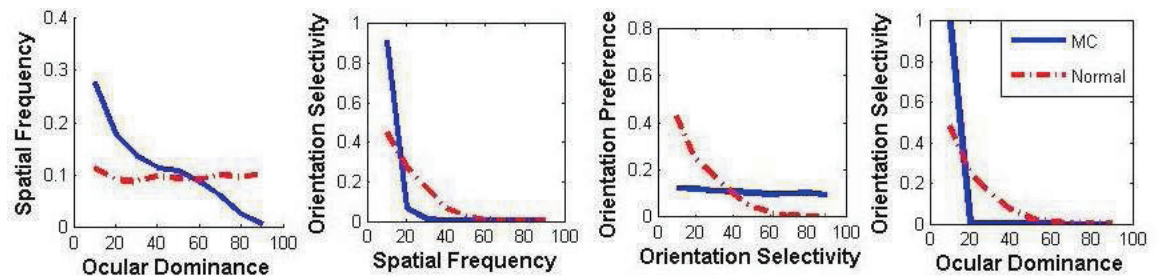


Figure 8: Pixels of one specific feature map are grouped into ten bins according to their gradient percentile (x-axis), and the percentage of pixels (of a different feature map) for each percentile group is indicated (y-axis, shown as a fractional value out of 1).

### 3.5 General Observations: Disease Case 1 and 2

The injured maps of ocular dominance exhibited similar patterns in organization as did those of orientation selectivity and spatial frequency. However, the maps of orientation preference exhibited more uniform areas affected by retinal injury (Figure 6). For disease case 1 and 2, azimuth and elevation

retinotopic position maps did not exhibit any significant differences as compared to the retinotopic position maps formed under normal conditions<sup>6</sup>.

### 3.6 Disease Model with Monte Carlo (MC) Stimulus Sampling

The response features of orientation selectivity and spatial frequency were sampled according to a Gaussian normal probability distribution. This was done to model the prediction that during cases of retinal injury, relatively high values for orientation selectivity and spatial frequency would be represented less than lower values during feature map formation. The stimulus distribution values for orientation selectivity and spatial frequency are shown in figure 7.

### 3.7 Gradient relationships between response features: MC

Compared with gradient relationships for normal maps, in MC maps the same gradient relationships between certain response features are significantly different (Figure 8). This suggests that during cases of retinal injury in which spatial frequency and orientation selectivity map formation are affected for the entire visual field (and thereby affecting representation of these features for all associated neurons), certain gradient relationships between response features are affected as well. All of the gradient relationships analyzed are significantly changed in the MC model as compared with the normal model. The data strongly suggests that in cases where orientation selectivity and spatial frequency representation are affected, normal relationships among response features are affected significantly.

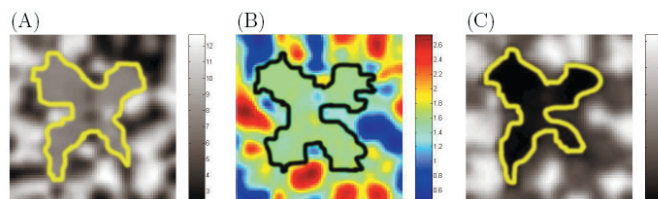
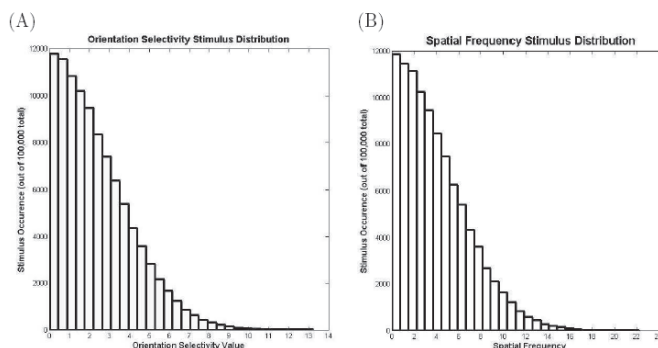


Figure 6: Cortical maps of (A) ocular dominance, (B) orientation preference, and (C) spatial frequency. Diseased areas in (A,B) are outlined. The diseased area in (C) is shaded. All images are from Disease Case 2, scattered, with injury radius of 15.



(Figure 7: MC disease case: Stimulus value distributions for (A) orientation selectivity and (B) spatial frequency. This distribution shows as the number of occurrences per interval out of 100,000 total stimuli values.

<sup>7</sup> See Appendix C for maps of other response features

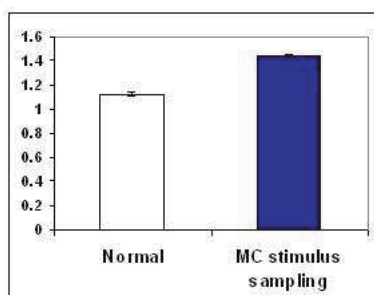


Figure 9: MC disease case: coverage uniformity comparison between normal and MC maps.

### 3.8 Coverage Uniformity Comparisons

Response feature maps formed under the MC disease case exhibited significantly higher coverage uniformity ( $c'$ ) values than did those formed under normal conditions ( $P < 0.0001$ ,  $n=10$ ,  $c'=1.44008$  for MC map,  $c'=1.12508$  for normal map) (Figure 9). The data suggests that the MC disease map is not optimized for uniform coverage. Coverage uniformity analysis was performed for disease cases 1 and 2, but the results did not exhibit significant differences between maps of different disease sizes<sup>7</sup>.

## 4 Discussion

In this investigation, it was shown that normal cortical maps can form even in the absence of visual input from small areas of the retina. It was found that retinal injuries with a radius less than 5 units did not impact the continuity in the formation of the cortical map. Cortical maps that were formed under both disease cases with radii of 2.5 units and 5 units retained similar structure to the map formed under normal conditions. Although there was a difference in the arrangement of intensity “blotches” (enclosed areas of the cortical map which represent neurons firing at similar intensities (e.g. blotches of red which represent neurons firing at high intensity) within the cortical maps of orientation selectivity for normal and diseased cases, the overall structure of diseased maps (disease radius 2.5 and 5) retained continuity.

Through analysis of differences between gradient magnitudes of normal and injured maps, it can be confirmed that the features of orientation selectivity, orientation preference, and ocular dominance are not affected dramatically with a disease of radius 2.5. However, with a disease of radius 2.5, spatial frequency maps are still affected significantly as compared with the normal feature map. This observation suggests that the spatial frequency feature map is affected even in situations in which the retinal disease size is small. Furthermore, it is evident that the spatial frequency feature is affected significantly following retinal injury. The results of gradient magnitude comparisons show significant differences in all features between the maps of disease radius 5 versus those of the normal map (which suggests that injury of radius 5 significantly affects response feature map formation.

However, gradient plots do not suggest a clear distinction between the normal and affected maps of disease radius 5. Further analysis is necessary to determine the effects of retinal disease of radius 5.

The concept of continuity is pivotal in interpreting the results of this investigation. In this investigation, continuity refers to “the desire to represent all input features smoothly” [2]. In (Figure 2A) the center area is continuous because the neurons in the center primarily fire at intensities on the higher end or the lower end; this pattern is represented throughout the entire cortical map. However, in (Figure 2C) the center area is not continuous because the neurons primarily fire at the same intensity as during initial conditions. These neurons primarily fire in the middle of the range of possible intensities; this pattern is different from those which are exhibited in other areas of the map.

Coverage uniformity is also important in interpreting the effects of retinal disease [14]. Since it has been shown that cortical maps optimize (i.e. minimize) coverage uniformity, we predicted that diseased maps would show a higher, less optimal coverage uniformity. Our hypothesis was substantiated in the MC disease case but not in disease cases 1 and 2, for which only certain areas of the visual cortex were affected.

Previous studies have shown that certain response features bear strong relationships with each other [1, 5, 7, 11, 12]. It has been shown that there is a strong negative correlation between the map formations of orientation preference and spatial frequency. Furthermore, it has been found that the representation of orientation preference map formation influenced the representation of ocular dominance map formation [3]. Based on these data, Yu et al. proposed that the following combinations of response features are represented such that one feature influences the other: orientation preference and orientation selectivity, orientation selectivity and spatial frequency, orientation selectivity and ocular dominance. It can be hypothesized that since certain features influence the formation of response feature maps of other features, the elimination of a feature from the study could impact the maps of other response features. It can also be proposed that the feature maps which formed as a result of elimination of other features will form differently in the presence of a retinal injury. Future studies should investigate these concepts.

Future models of retinal disease should manipulate the features of orientation selectivity and spatial frequency. Although it was hypothesized that orientation selectivity representation would be strongly affected by retinal disease, results of analysis for disease cases 1 and 2 do not provide conclusive evidence that orientation selectivity is substantially affected by retinal disease. The MC disease case models the prediction that representation of orientation selectivity and spatial frequency would be strongly affected by retinal disease. Since results of disease cases 1 and 2 suggest that orientation selectivity representation is not strongly affected by retinal disease, experimental studies should be conducted which confirm this observation.

<sup>7</sup> For disease cases 1 and 2, since only the affected areas were analyzed for coverage uniformity, we propose that the lack of a general trend in coverage uniformity differences was due in part to the lack of variability of represented stimuli values in the injured areas.



## 5 Conclusion

This study suggests that small retinal injuries may not necessarily impact the function of the primary visual cortex in adapting to visual input. This study also suggests that certain response features are represented differently in terms of neuronal activity in the primary visual cortex. Lastly, this study shows that certain relationships between response features are preserved after retinal injury. The results of this study can be confirmed by studies analyzing the electrophysiological responses in areas of the visual cortex analogous to the affected visual field. This investigation serves as a predicative model for future experiments regarding response feature map formation in response to stimuli distributions as well as stimuli locations as exhibited in retinal disease. Furthermore, the results of this study can be applied to the development of possible treatments for disease in the primary visual cortex as well as in the broader neocortex.

## Acknowledgements

I would like to thank my mentor, Dr. Dezhe Jin, for his insightful guidance and support during the course of this project. Furthermore, I would like to thank Mr. Srinivas Turaga, who provided me with conceptual explanations and advice on furthering the development of my project. Also, I would like to thank Dr. Jenny Sendova for helping me with my scientific writing and presentation skills.



## References

- [1] A. Basole, L.E. White, D. Fitzpatrick. Mapping multiple features in the population response of visual cortex. *Nature*. 26 Jun 2003; 423(6943):986-90.
- [2] M.A. Carreira-Perpinan and G.J. Goodhill. Influence of Lateral Connections on the Structure of Cortical Maps. *Journal of Neurophysiology*. 2 June 2004; 92:2947-2959.
- [3] H. Yu, B.J. Farley, D.Z. Jin, and M. Sur. The Coordinated Mapping of Visual Space and Response Features in Visual Cortex. *Neuron*. 21 July 2005; 47(2):267-80.
- [4] T. Germano. Self Organizing Maps. Available at <http://davis/wpi.edu/~matt/courses/soms/> (25 July 2006)
- [5] N.P. Issa, C. Trepel, and M.P. Stryker. Spatial frequency maps in cat visual cortex. *Journal of Neuroscience*. 15 Nov 2000; 20(22):8504-14.
- [6] A.A. Koulakov and D.B. Chklovskii. Orientation preference patterns in mammalian visual cortex: a wire length minimization approach. *Neuron*. Feb 2001; 29(2):519-27.
- [7] V. Mante and M. Carandini. Mapping of stimulus energy in primary visual cortex. *Journal of Neurophysiology*. July 2005; 94(1):788-98.
- [8] Neural Networks Research Group. The Primary Visual Cortex. Available at <http://nn.cs.utexas.edu/web-pubs/sirosh/pvc.html> (08 July 2006).
- [9] S.C. Rao, L.J. Toth, and M. Sur. Optically imaged maps of orientation preference in primary visual cortex of cats and ferrets. *The Journal of Comparative Neurology*. 27 Oct 1997; 387(3):358-370.
- [10] I.A. Rybak, L.N. Podladchikova, N.A. Shevtsova, and A.V. Golovan. Experimental Study and Computational Modeling of Orientation Selectivity in the Visual Cortex. Available at <http://www.rybak-et-al.net/iod.html> (30 July 2006)

- [11] L. Sirovich and R. Uglyich. The organization of orientation and spatial frequency in primary visual cortex. *Proceedings of the National Academy of Sciences - USA*. 30 Nov 2004; 101(48):16941-6.
- [12] N.V. Swindale. How different feature spaces may be represented in cortical maps. *Network*. Nov 2004; 15(4):217-42.
- [13] S. Zeki. *A vision of the brain*. Blackwell Scientific Publications, London, England (1993).
- [14] N.V. Swindale, D. Shoham, A. Grinvald, T. Bonhoeffer, and M. Hubener. Visual cortex maps are optimized for uniform coverage. *Nature neuroscience*. August 2000, vol. 3, no. 8.

## Appendices

### A Definitions

The response features of the visual cortex include: orientation preference, orientation selectivity, spatial frequency, and ocular dominance.

**Orientation selectivity** is a feature which involves the detection of local bars and edges in the processed visual images, as well as their orientations [10].

**Orientation preference** refers to the angle of the presented stimulus at which the neurons respond most.

**Spatial frequency** refers to how much a periodic structure repeats per unit of distance in the visual field. For example, the sine-wave grating is used as a means for assessing spatial frequency. Sine-wave gratings which appear blurry have low spatial frequency; distinct, clear sine-wave gratings have high spatial frequency [13].

**Ocular dominance** refers to the preference to receive visual input from a particular eye. Low values for ocular dominance indicate the preference to receive input from the contralateral eye, while high values indicate preference to receive input from the ipsilateral eye. [13].

### B Gradient Magnitude Comparison Results

Tables 1-8 show the gradient magnitude comparisons, which were performed with unpaired t-tests. A \* denotes a significant difference between normal and injured maps. Tables 1-4 display results from disease case 1, while tables 5-8 display results from disease case 2.



Table 1: Disease Case 1: Orientation Selectivity

| Disease Radius | Average Gradient Magnitude - Normal | Average Gradient Magnitude - Injured | P-value       |
|----------------|-------------------------------------|--------------------------------------|---------------|
| 2.5            | 0.6983                              | 0.2498                               | 0.0755        |
| 5              | 0.5175                              | 0.4115                               | 0.0425*       |
| 15             | 0.4370                              | 0.2032                               | $P < 0.0001*$ |

Table 2: Disease Case 1: Orientation Preference

| Disease Radius | Average Gradient Magnitude - Normal | Average Gradient Magnitude - Injured | P-value       |
|----------------|-------------------------------------|--------------------------------------|---------------|
| 2.5            | 0.2270                              | 0.1857                               | 0.1170        |
| 5              | 0.2167                              | 0.1471                               | $P < 0.0001*$ |
| 15             | 0.1672                              | 0.0762                               | $P < 0.0001*$ |

Table 3: Disease Case 1: Spatial Frequency

| Disease Radius | Average Gradient Magnitude - Normal | Average Gradient Magnitude - Injured | P-value       |
|----------------|-------------------------------------|--------------------------------------|---------------|
| 2.5            | 1.5463                              | 0.1471                               | $P < 0.0001*$ |
| 5              | 1.1631                              | 1.5569                               | 0.0004*       |
| 15             | 1.2174                              | 0.7707                               | $P < 0.0001*$ |

Table 4: Disease Case 1: Ocular Dominance

| Disease Radius | Average Gradient Magnitude - Normal | Average Gradient Magnitude - Injured | P-value       |
|----------------|-------------------------------------|--------------------------------------|---------------|
| 2.5            | 0.7884                              | 0.6838                               | 0.2067        |
| 5              | 0.7977                              | 1.5569                               | $P < 0.0001*$ |
| 15             | 1.0450                              | 0.5457                               | $P < 0.0001*$ |

Table 5: Disease Case 2: Orientation Selectivity

| Disease Radius | Average Gradient Magnitude - Normal | Average Gradient Magnitude - Injured | P-value       |
|----------------|-------------------------------------|--------------------------------------|---------------|
| 2.5            | 0.3724                              | 0.3960                               | 0.4422        |
| 5              | 0.4021                              | 0.3506                               | 0.0010*       |
| 15             | 0.4191                              | 0.3104                               | $P < 0.0001*$ |

Table 6: Disease Case 2: Orientation Preference

| Disease Radius | Average Gradient Magnitude - Normal | Average Gradient Magnitude - Injured | P-value       |
|----------------|-------------------------------------|--------------------------------------|---------------|
| 2.5            | 0.1418                              | 0.1765                               | 0.0623        |
| 5              | 0.1678                              | 0.1402                               | 0.0071*       |
| 15             | 0.1748                              | 0.1014                               | $P < 0.0001*$ |

Table 7: Disease Case 2: Spatial Frequency

| Disease Radius | Average Gradient Magnitude - Normal | Average Gradient Magnitude - Injured | P-value       |
|----------------|-------------------------------------|--------------------------------------|---------------|
| 2.5            | 1.3190                              | 0.9359                               | $P < 0.0001*$ |
| 5              | 1.1443                              | 0.9413                               | $P < 0.0001*$ |
| 15             | 1.0827                              | 0.6916                               | $P < 0.0001*$ |

Table 8: Disease Case 2: Ocular Dominance

| Disease Radius | Average Gradient Magnitude - Normal | Average Gradient Magnitude - Injured | P-value       |
|----------------|-------------------------------------|--------------------------------------|---------------|
| 2.5            | 0.9562                              | 0.6770                               | 0.0590        |
| 5              | 0.8595                              | 0.6702                               | 0.0235*       |
| 15             | 1.0309                              | 0.6971                               | $P < 0.0001*$ |

### C Response Feature Maps After Injury

The following response feature maps were obtained for disease cases 1 and 2. The response feature maps for all features exhibited similar patterns. All injuries of radius 2.5 and 5 did not significantly impact continuity in the formation of cortical response feature maps.

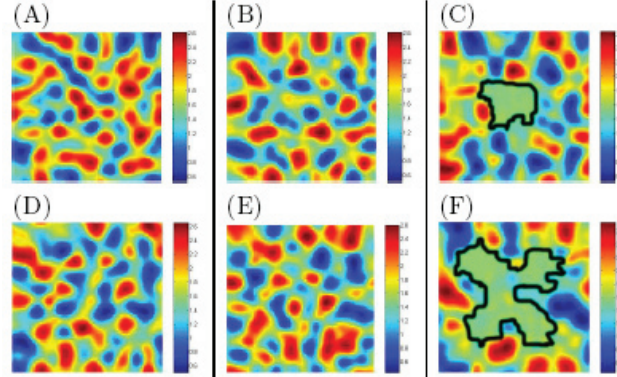


Figure 10: Cortical maps of orientation preference, with diseases of radius 2.5 (A,D), 5 (B,E), and 15 units(C,F).

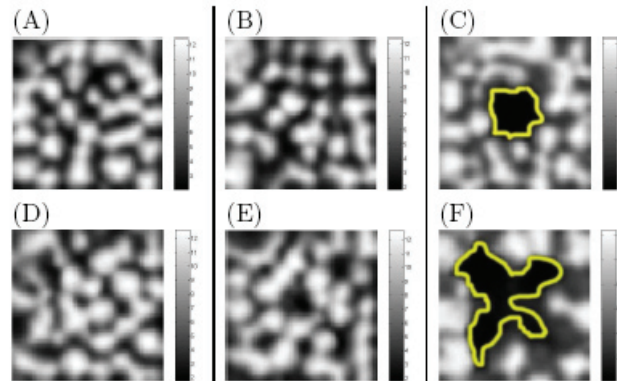


Figure 11: Cortical maps of spatial frequency, with diseases of radius 2.5 (A,D), 5 (B,E), and 15 units(C,F).

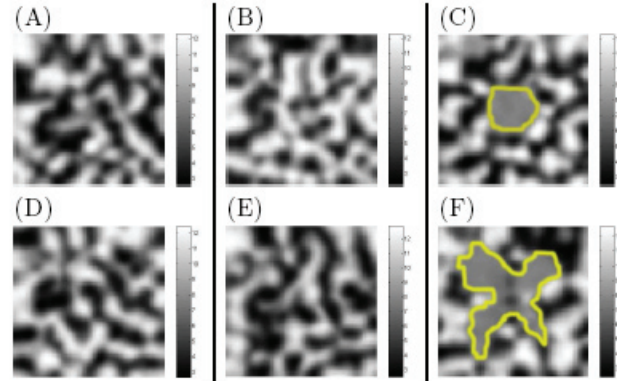


Figure 12: Cortical maps of ocular dominance, with diseases of radius 2.5 (A, D), 5 (B, E), and 15 units (C, F).